Assessment of Various Bias Correction Methods on Precipitation of Regional Climate Model and Future Projection

Gunavathi S

SASTRA University School of Civil Engineering: Shanmugha Arts Science Technology and Research Academy School of Civil Engineering

Selvasidhu R (selvakumar@civil.sastra.edu)

SASTRA University School of Civil Engineering: Shanmugha Arts Science Technology and Research Academy School of Civil Engineering https://orcid.org/0000-0002-1635-8977

Research Article

Keywords: CORDEX, Precipitation, Future projection, Bias correction, Power transformation method, Thanjavur district

Posted Date: April 7th, 2021

DOI: https://doi.org/10.21203/rs.3.rs-339080/v1

Corresponding Author: Selvakumar Radhakrishnan

ASSESSMENT OF VARIOUS BIAS CORRECTION METHODS ON PRECIPITATION OF REGIONAL CLIMATE MODEL AND FUTURE PROJECTION

Gunavathi S[1]., Selvakumar Radhakrishnan[2]

[1, 2] School of Civil Engineering, SASTRA Deemed to be University, Thanjavur, Tamil Nadu, India.
Email id[2]: selvakumar@civil.sastra.edu

Abstract:

The application of regional climate model simulations (RCMs) in climate change impact studies is challengeable due to the risk of possible biases. Some sort of correction needs to be done prior to the application of RCM simulations. This study attempts to assess the performance of a simple (linear scaling and Delta Change method) and complex correction technique (Local intensity scaling, Power transformation and Distribution mapping) on CORDEX(Coordinated Regional Climate Downscaling Experiment)simulated precipitation series for the Thanjavur district. The performance at annual resolution is evaluated using various statistical parameters such as Correlation, Root Mean Square Error and Bias against the observed precipitation data. The raw RCM estimates were improved significantly after the bias correction with all methods. However, Power transformation exhibits good agreement with the observed data at the district level than other methods because it corrects both the mean and variance. The future climate was projected from 2021 to 2100 for RCP 4.5 and RCP 8.5 scenarios. The temporal distribution of future precipitation clearly shows that most of the years will receive heavy precipitation; rather, some years will receive low and average precipitation. The spatial distribution pattern indicates that the northeast monsoon will dominate over all the ranges and places. This study has provided clear information on future precipitation to the environmentalist, urban planners, and policymakers to take appropriate mitigation measures towards agriculture and disaster management. Rainwater harvesting, recharging the aquifers, afforestation, and redirecting the excess amount of water to the river through proper channels is the plausible actions suggested overcoming excessive precipitation in the future.

Keywords: CORDEX, Precipitation, Future projection, Bias correction, Power transformation method, Thanjavur district

1.0 Introduction:

Climate change, a complex phenomenon and critical issue being faced by the earth, has posed immense threats to the ecological and human environment. The Intergovernmental Panel on Climate Change (IPCC) reported that in the past few decades, global temperature, precipitation patterns and the occurrence of disasters such as cyclones, droughts, floods and heatwaves had risen notably in terms of both frequency and severity (IPCC 2013; Prusty et al. 2018). Though climate change is a long-term event, its impact may be imperceptibly gradual and steady. Therefore, evaluating its effects and susceptibility to adaptation requires better knowledge about the future climate. The research community worldwide is currently using coarse and high-resolution climate models for climate predictions and assessment (Giorgi et al. 2018). In general, the course resolution Global Climate Models (GCMs) has shortcomings in capturing regional orographic characteristics. In contrast, high-resolution Regional Climate Models (RCMs) reflect improved orography and generate more accurate climate projection. Hence commonly used to evaluate the past, present and future climates across the world (Kumar et al. 2013).

Accordingly, the Coordinated Regional Climate Downscaling Experiment (CORDEX), a coordinated initiative involving several countries worldwide, produces various regional and local climate simulations (Giorgi et al. 2009). Even though RCM simulations are driven using multiple GCMs with the improved horizontal resolution, it yields errors. Biases are due to the uncertainty in physical parameterizations, lateral boundary conditions, initial condition limitation, numerical model imperfectness, and so on (Giorgi et al. 1999; Christensen et al. 2008; Rauscher et al. 2010; Hall et al. 2014). In consequence, reduces the reliability and increases the uncertainty in using the RCM simulations directly as input data for climate change studies (Noguer et al. 1998). However, earlier studies have concluded that the climate model outputs shall be refined by applying statistical corrections (Veijalainen et al. 2010; Dosio et al. 2011; Hanel et al. 2011; Monhart et al. 2018; Pontoppidan et al. 2018). Researchers use multiple bias correction methods for reducing model errors and also to downscale the GCM data. The techniques vary from basic scaling to very complex methods like weather generators, probability mapping, etc. Overall, bias correction methods use the transformation algorithm for correcting the RCMs output by identifying the bias between observed and simulated data. The derived bias correction algorithm and parameterization are also used to correct the RCM projection scenarios (Chen et al. 2011b; Johnson et al. 2011).

In general, corrections are made by correcting the mean, wet day frequencies and percentile on the simulated data with reference to the observed data (Gudmundsson et al. 2012; Teutschbein et al. 2012, 2013; Chen et al. 2013). Based on the mean, standard deviation, and coefficient of variation of the observed data, Terink et al. (2009) adjusted the daily RCM-simulated precipitation and temperature data for the Rhine basin. The distribution mapping method was used to adjust the RCM simulated daily precipitation dataset over Europe and found that this method worked relatively well under normal and extreme conditions (Piani et al. 2010). Themeßl et al. (2012) found that quantile mapping and local intensity scaling (LOCI) methods effectively correct the Alpine region's daily precipitation simulation by analyzing seven bias correction techniques. Similarly, Bennett et al. (2011) also used quantile mapping to correct annual and seasonal RCM rainfall deviations in Australia and noted an improved spatial distribution after correction. To reduce the bias of RCM-simulated precipitation for seven catchments across the United Kingdom, Lafon et al. (2013) assessed linear, nonlinear, gamma and quantile mapping based on empirical distribution methods. The RCM simulated precipitation dataset has also been corrected using distribution, parametric and nonparametric transformations for 83 stations in Norway by Gudmundsson et al. (2012). N'Tcha M'Po et al. (2016) found that the empirical-based quantile mapping approach works better than Gamma-based quantile mapping to correct extreme precipitation. Three distinct processes, such as linear scaling, regression and empirical quantile mapping, were compared to select the most effective method over the Northwest Himalayas using four statistical measurements by Devi et al. (2021). Thus, most research is conducted to identify the best method that shows good agreement with observed data. Accordingly, in the present study, linear scaling, local intensity scaling, power transformation, distribution mapping, and delta-change methods are evaluated on REMO 2009 RCM. The projection of precipitation using the best bias correction method RCP 4.5 and RCP 8.5 scenarios is carried out.

2.0 Study area:

Thanjavur district located between 9º 50' and 11º 25' North and 78º 45' and 79º 25' East with the total geographical area of 3,602.86 sq. km has been studied. The region possesses three rainy seasons such as

summer rain (March-May), South-West monsoon (June-September) and North-East monsoon (October-Early January). Amongst, the North-East monsoon (545.7 mm of normal rainfall) and the South-West monsoon (342 mm of normal rainfall) plays a significant role in feeding the river Cauvery, the primary source of irrigation of the study area. The area is unique for its agricultural activities from time immemorial and is renowned as the granary of South India. Besides the river Cauvery, the area has been crisscrossed by a network of irrigation channels. Hence, this coastal district is flourishing in paddy fields, coconut and mango groves, plantain trees and other vegetation. However, in recent times, agriculture seems to get destabilized due to uncertain climatic conditions. The study area map shows 14 blocks with 17 well-distributed rain gauge stations around the district (Figure1).

3.0 Materials and Methods:

The four steps methodology has adopted in this study (Figure 2).

3.1 Collection of observed and model data:

In this study, the daily precipitation data were collected for 30 years (1976 – 2005) from the Indian Meteorological Department (IMD). The obtained data was found with some gaps. Hence observed proxy data (APHRODITE - Asian Precipitation – Highly –Resolved Observational Data Integration Towards Evaluation) (http://aphrodite.st.hirosaki-u.ac.jp/) and reanalysis data (ERA - INTERIM) (https://apps.ecmwf.int/datasets/data/interim-full-daily/levtype=sfc/) were collected, and the annual mean compared against the observed data. In that, APHRODITE data has shown a high correlation of 0.73 with the observed data. Thus, observed IMD data was primarily used in the present study, while the data gaps were filled with APHRODITE data.

CORDEX is a global programme for localized climate change scenarios. CORDEX South Asia domain experiment consists of eleven distinct suites, with different RCMs driven by various initial and boundary forcing GCMs. Within the context of CORDEX, the Max Planck Institute for Meteorology is extending its regional climate model REMO to many regions of the planet. This study employed the daily precipitation datasets of the REMO 2009 simulations driven by the MPI-MPI-ESM-LR driving model of CORDEX-SOUTH ASIA domain (WAS-44i; ~50 km horizontal resolution). The data is available in the Earth Systems Grid Federation (ESGF) under the CORDEX project (https://esgf-index1.ceda.ac.uk/search/esgf-ceda/).

3.2 Selection of bias correction techniques:

As stated earlier, datasets were collected on daily observed data (IMD) and RCM Simulated precipitation for a control period of 30 years (1976–2005) for bias correction. Hereafter, the RCM simulated data for the historical period will be called 'control data' and for the future period as 'scenario data'. Amongst various bias correction methods, the following were used to adjust the control data in the present study (1) linear scaling, (2) local intensity scaling, (3) power transformation, (4) distribution mapping and (5) delta-change approach.

3.2.1 Linear scaling of precipitation (LS):

LS is the most straightforward bias correction technique employed in several studies (Ines et al. 2006; Teutschbein et al. 2012; Shrestha et al. 2015). It adjusts the RCM mean value with a perfect agreement with the observation data. The control and scenario precipitation are then adjusted based on the ratio between the long-term monthly mean observed and control/scenario data using equations (1) and (2), respectively. However, this approach can correctly adjust the climatic factors only when the monthly mean values are included.

$$P^{*}_{control}(d) = P_{control}(d) \cdot \left[\frac{\mu_m \left(P_{observed}(d) \right)}{\mu_m \left(P_{control}(d) \right)} \right] \quad (1)$$

$$P^{*}_{scenario}(d) = P_{scenario}(d) \cdot \left[\frac{\mu_m \left(P_{observed}(d) \right)}{\mu_m \left(P_{control}(d) \right)} \right] \quad (2)$$

Where, P = precipitation; (d) = daily time series; μ = mean and P^* = final bias corrected.

3.2.2 Local intensity scaling (LOCI) of precipitation:

The LOCI method introduced by Schmidli et al. (2006) extends the linear scaling method a step forward. Added to the mean, it also adjusts wet-day frequencies and wet-day intensities of precipitation. The precipitation intensity threshold (Pth, control) for every month is initially confirmed. Then, the number of wet days in control data that exceeds the threshold will be adjusted based on the number of days the observed precipitation was determined. The number of precipitation events for control and scenario run is corrected by applying the calibrated RCM precipitation threshold (Pth, control) using Equations (3) and (4), respectively. This approach virtually eliminates the drizzle effect because excessive drizzly days are frequently added to the RCM outputs.

$$P^{*1}_{control}(d) = \begin{cases} 0, & \text{if} \quad P_{control}(d) < P_{th,control} \\ P_{control}(d), & otherwise \end{cases} \tag{3}$$

$$P^{*1}_{scenario}(d) = \begin{cases} 0, & \text{if} \quad P_{scenario}(d) < P_{th,control} \\ P_{scenario}(d), & otherwise \end{cases} \tag{4}$$

A scaling factor s is then calculated using equation (5) to confirm that the mean of corrected precipitation is equal to observed data.

$$s = \frac{\mu_m\left(P_{observed}(d) \middle| P_{observed}(d) > 0 \text{ mm}\right)}{\mu_m\left(P_{control}(d) \middle| P_{control}(d) > P_{th,control}\right) - P_{th.control}} \tag{5}$$

Finally, both control and scenario precipitations are corrected using equation (6) and (7), respectively.

$$P^{*}_{control}(d) = P^{*1}_{control}(d) \cdot s \tag{6}$$

$$P^{*}_{scenario}(d) = P^{*1}_{scenario}(d) \cdot s \tag{7}$$

Where, th = threshold and P^{*1} = intermediate step in bias correction.

3.2.3 Power transformation of precipitation (PT):

PT corrects both the monthly mean as well as the variance. It uses an exponential correcting factor aP^b (Mendez et al. 2020; Kim et al. 2020). Parameter 'b' is measured monthly (b_m) using the distribution-free method with a three-month window. Initially, 'b' is determined by equalizing the Coefficient of Variation (CV) of corrected RCM precipitation (P^b) and observed precipitation ($P_{observed}$) for every month (m) using the root-finding algorithm (Brent 1971). Then 'b_m' is calculated using equation eight and 'CV_m' using equation nine. Equation 10 & 11 were used for equalizing the datasets.

$$f(b_m) = 0 = CV_m\left(P_{observed}(d)\right) - CV_m\left(P^{b_m}_{control}(d)\right) \tag{8}$$

$$\frac{\sigma_m\left(P_{observed}(d)\right)}{\mu_m\left(P_{observed}(d)\right)} - \frac{\sigma_m\left(P^{b_m}_{control}(d)\right)}{\mu_m\left(P^{b_m}_{control}(d)\right)} \tag{9}$$

$$P^{*1}_{control}(d) = P^{b_m}_{control}(d) \tag{10}$$

$$P^{*1}_{scenario}(d) = P^{b_m}_{scenario}(d) \quad (11)$$

Afterwards, 'PT' equalizes the observed precipitation ($P_{observed}$) with the intermediate series ($P^{*1}_{control}$) using the LS method. Finally, the corrected control and scenario precipitation datasets were derived using equations 12 and 13, respectively.

$$P^{*}_{control}(d) = P^{*1}_{control}(d) \cdot \left[\frac{\mu_m\left(P_{observed}(d)\right)}{\mu_m\left(P^{*1}_{control}(d)\right)} \right] \quad (12)$$

$$P^{*}_{scenario}(d) = P^{*1}_{scenario}(d) \cdot \left[\frac{\mu_m\left(P_{observed}(d)\right)}{\mu_m\left(P^{*1}_{control}(d)\right)} \right] \quad (13)$$

3.2.4 Distribution mapping of precipitation (DM):

The DM method is applied to correct mean, standard deviation (SD), and quantiles by equalizing the distribution functions of both the RCM outputs and the observed data. The method assumes that the RCM-simulated and observed precipitation follows a particular frequency of distribution, in turn, may cause biases (Themeßl et al., 2012). Accordingly, Gamma distribution was used for effective precipitation distribution.

$$f_\gamma\left(\chi \middle| \alpha, \beta\right) = \chi^{\alpha-1} \cdot \frac{1}{\beta^\alpha \cdot \Gamma(\alpha)} \cdot e^{\frac{-\chi}{\beta}}; \chi \geq 0; \qquad \alpha, \beta > 0 \quad (14)$$

Where Γ(.) is the Gamma function, α is the shape parameter, and β is the scale parameter. Before the DM method, the LOCI method is applied to determine the wet days using the specific threshold. Subsequently, RCM outputs were corrected in terms of the Gamma cumulative distribution function (F_γ) and its inverse function ($F^{-1}{}_\gamma$) as follows:

$$P^{*}_{control}(d) = F^{-1}_{\gamma}\left(F_\gamma\left(P_{control}(d) \middle| \alpha_{control,m}, \beta_{control,m}\right) \middle| \alpha_{observed,m}, \beta_{observed,m}\right) \quad (15)$$

$$P^{*}_{scenario}(d) = F^{-1}_{\gamma}\left(F_\gamma\left(P_{scenario}(d) \middle| \alpha_{control,m}, \beta_{control,m}\right) \middle| \alpha_{observed,m}, \beta_{observed,m}\right) \quad (16)$$

3.2.5 Delta Change Method (DC):

DC method is comparatively simple and widely used (Middelkoop et al. 2001; Raty et al. 2014). The difference between the mean of the scenario and the control data is calculated. This change/delta is added with the monthly mean of observed data to compute the future projections using a multiplier factor (Equation18). As a result, the monthly distribution's shape is preserved, and the delta shifts the values. This approach does not allow for changes in extreme precipitation events due to its simple transfer function (Mendez et al. 2020). A multiplicative correction is used for the precipitation correction equation.

$$P^{*}_{control}(d) = P_{observed}(d) \quad (17)$$

$$P^{*}_{scenario}(d) = P_{observed}(d) \cdot \left[\frac{\mu_m\left(P_{scenario}(d)\right)}{\mu_m\left(P_{control}(d)\right)} \right] \quad (18)$$

3.3 Future Projection of Precipitation:

Climate projections are based on the emission scenarios, so-called Radiative Concentration Pathways (RCP), reflecting a shift in the radiative forcing at the atmosphere by 2100 compared to pre-industrial times (Van Vuuren et al. 2011a). The four RCPs (RCP2.6, RCP4.5, RCP6, and RCP 8.5) are named based on the radiative forcing change by 2100 (+ 2.6, + 4.5, + 6.0, and + 8.5 W/m2) respectively. In this study, CORDEX – REMO 2009 RCP 4.5 and RCP 8.5 were used for precipitation projection. The collected data were preprocessed using Climate Data Operators (CDO 2019) and bias-correction using CMhyd software (Rathjens et al. 2016).

4.0 Results & Discussion:

4.1 Performance assessment of various bias correction methods on the control data:

After bias correction, the annual mean was calculated for both observed and bias-corrected control datasets. Subsequently, a correlation was computed amongst them, and the same is shown in Figure 3. The figure shows that the DC method adjusted control data has an absolute agreement with observed data. The agreement is since the method equalizes the mean of both observed and adjusted control data. The LS and PT method yield the least bias amongst the other methods, while the LOCI method underestimated the inter-annual variability in all locations.

On the contrary, the DM method has shown a varied result. It has overestimated the inter-annual variability at many locations, while in a few places, it has underestimated and in some areas demonstrated a fair agreement. Thus, all the bias correction methods can improve the spatial statistics of simulated mean precipitation is inferred.

The Root Mean Square Error (RMSE) and biases were calculated (Table 1). RMSE estimates the standard deviation of the error distribution between the observed and adjusted control data. The DC method seems to yield no error from the results, while the PT and LS methods with significantly less deviation of 0.059 and 0.063, respectively. Conversely, the DM method has shown a moderate deviation (24.097) and the LOCI method with a very high deviation (105.144). Thus it can be surmised that the PT bias correction method shows better performance than others.

The bias indicates the difference between the adjusted control data and the observed data. Again the DC method seems to be with no biases. LS method reduces the precipitation amount by 0.04 mm, and PT represents negative bias, reducing the precipitation amount by 0.07 mm. The LOCI method also shows a strong negative bias, which reduces the amount of precipitation by 97.76 mm. In contrast, the DM method yields a strong positive bias, increasing the precipitation amount by 31.04 mm. Based on the bias calculation, it is presumed that the LS method is better for bias correction, followed by the PT method.

Thus from the above analyses, the DC approach should be neglected for assessment because it has equalled the observation with the current condition. Similarly, LOCI and DM methods were also to be avoided owing to their over and underestimations. Both LS and PT methods have shown a good agreement with observed data almost in all the analyses. Though LS accounts for the mean biases, it does not correct the biases in the variance. Thus it can be surmised that the PT approach can be adapted to adjust the future projections in the study.

Bias Correction Methods	RMSE	Bias
Linear scaling	0.063	-0.044
Local intensity scaling	105.144	-97.758
Power transformation of precipitation	0.059	-0.073
Distribution mapping	24.097	31.039
Delta change	0.000	0.000

Table 1. showing the root mean square error and bias for various bias correction methods

4.2 Projections using bias-corrected precipitation in RCP scenario:

The biases in RCP 4.5 and 8.5 scenario data were corrected using the PT method. Subsequently, grouped into three groups as the near range (2021 to 2050), mid-range (2051 to 2075), and far range (2076 to 2100).

4.2.1 Comparison between observed and adjusted control data (1976 – 2005):

Initially, the PT method's performance was evaluated by carrying out statistical analysis between the observed and adjusted control data. The result shows that the model underestimates the intensity of the precipitation until 1985 and then after exhibits both overestimation and good agreement with the observed data collectively (Figure 4). Similarly, a mean positive deviation of 38.96% and a negative deviation of 23% are witnessed between observed and adjusted control data (Table 2). Overall the model overestimates 14 times and underestimates 16 times the intensity of precipitation in the 30-year time series. However, though the frequency of negative deviation is higher, the intensity of precipitation it underestimates is lesser than the overestimation (Table 2).

Analysis	**Obs vs adjusted control**	**Obs vs near4.5**	**Obs vs mid4.5**	**Obs vs far4.5**	**Obs vs near8.5**	**Obs vs mid8.5**	**Obs vs far8.5**
Mean of Positive deviation	38.96%	63.02%	54.35%	56.73%	80.85%	54.41%	83.85%
(frequency)	(14)	(18)	(17)	(18)	(18)	(15)	(18)
Mean of Negative deviation	-23%	-22%	-28%	-26%	-23%	-24%	-19%
(frequency)	(16)	(12)	(8)	(7)	(12)	(10)	(7)
Analysis	**Adjusted control vs near4.5**	**Adjusted control vs mid4.5**	**Adjusted control vs far4.5**	**Adjusted control vs near8.5**	**Adjusted control vs mid8.5**	**Adjusted control vs far8.5**	
Mean of Positive deviation	65.84%	91.73%	61.94%	66.02%	55.68%	81.16%	
(frequency)	(20)	(15)	(17)	(20)	(15)	(18)	
Mean of Negative deviation	-25%	-27%	-26%	-27%	-26%	-24%	
(frequency)	(10)	(10)	(8)	(10)	(10)	(7)	

Table 2. Comparison of adjusted scenario data with observed and bias corrected control data

4.2.2 The near range (2021 – 2050) of RCP 4.5 and RCP 8.5:

In general, precipitation shows an increase during the first decade and then after a gradual decrease in both scenarios (Figure 4). The RCP 4.5 has shown higher precipitation during 2022, 2025, 2031 and 2033 while RCP 8.5 during 2027, 2039 and 2048. The calculated bias denotes that precipitation has increased by 80.99 mm in RCP 8.5 with an occurrence frequency of 17 than RCP 4.5 (Figure 5). Meanwhile, the comparison with observed data shows increased precipitation in both RCP 4.5 (63.02%) and RCP 8.5 (80.85%) but with the same number of occurrences (18). Similarly, an increase of 65.84% for the RCP 4.5 scenario and 66.02% for RCP 8.5 with the same number of occurrences (20) is noticed with adjusted control data for 30 years time series (Table 2).

The spatial distribution of annual mean precipitation for both scenarios in the near range is represented in figure 6 and figure 7. In RCP 4.5, most of the area receives precipitation of around 1150 mm. However, a decrease in the west and increases towards the northeast is also noticed. The RCP 8.5 exhibits a similar spatial pattern; however, most places have shown relatively increased precipitation of about ~1275 mm (Figure 6). From the wind rose diagram (Figure 7), it is witnessed that Manjalar head and Lower anaicut area receives higher precipitation (~ 1600 mm) whereas Grand anaicut and Thirukattupalli area with lower precipitation (~ 1000 mm).

Overall, higher precipitation of RCP 8.5 is attributed to radiative forcing. But the frequency of occurrence seems to be similar for both RCP scenarios as far observed and adjusted control data is concerned. The same is attributed to the effect of the adapted bias correction method.

4.2.3 The mid range (2051 – 2075) of RCP 4.5 and RCP 8.5:

It is found that RCP 4.5 receives higher precipitation during 2052, 2056 and 2065, while RCP 8.5 receives more precipitation during the years 2053 and 2057. Based on the calculated bias, the amount of precipitation seems to have increased by 99.19 mm in RCP 4.5 with an occurrence frequency of 12 compared to RCP 8.5 (Figure 5). Similarly, the comparison with the observed data shows that RCP 4.5 yields an increased amount of precipitation (54.35%) with a frequency rate of 17. In contrast, RCP 8.5 possesses 54.41% of increased precipitation with a

frequency rate of 15. The adjusted control data increases 91.73% for the RCP4.5 scenario, while the RCP 8.5 shows an increase of 55.68% with the same number of occurrences (15) for the 25 years time series (Table 2).

The spatial distribution of annual mean precipitation for both scenarios in the mid range is represented in figure 7 and figure 8. In RCP 4.5, the Adhiramapattinam, Lower anaicut, Manjalar head, and Pattukottai receive more precipitation (~1400 mm), whereas Grand anaicut and Thirukattupalli receives low precipitation (~1000 mm). While in RCP 8.5, the Lower anaicut, Manjalar head, Pattukottai, Papanasam, Kumbakonam, Vetticadu and Thanjavur receives high precipitation (~1300 mm), and Thiruvaiyaaru, Grand anaicut and Thirukattupalli receives low precipitation (~1100 mm).

Overall, it is found that the mid-range of RCP 4.5 receives higher precipitation than RCP 8.5. Thus, it is inferred that the radiative forcing does not influence the intensity of the precipitation.

4.2.4 The far range (2076 – 2100) of RCP 4.5 and RCP 8.5:

The projected precipitation is overestimated by RCP 8.5 in 2082 with an unrealistic amount of ~5000 mm (Figure 4). The precipitation intensity increases by 132.47 mm in RCP 8.5, with an occurrence frequency of 17 and receiving higher precipitation during 2082 and 2093. Whereas in RCP 4.5, higher precipitation is witnessed during 2090 and 2092 (Figure 5). RCP 4.5 yields an increased precipitation of 56.73%, whereas 83.85% is for the RCP 8.5 scenario with the same frequency rate (18) against observed data. Concerning adjusted control data, an increase of 61.94% with an occurrence rate of 17 for RCP4.5 and for RCP 8.5, 81.16% with a frequency of 18 is witnessed for 25 years time series (Table 2).

The spatial distributions of annual mean precipitation for both scenarios in the far range are represented in figure 7 and figure 9. Adhiramapattinam, Lower anaicut and Manjalar head shows high precipitation (~1400 mm), whereas Grand anaicut and Thirukattupalli with low precipitation (~ 1000 mm) in RCP 4.5. on the contrary, RCP 8.5 has shown a more significant variation in the distribution pattern with high precipitation (~1750 mm) in Lower anaicut, Manjalar head and Kumbakonam and low precipitation (~1100 mm) in Peravoorani, Thirukattipalli, and Grand anaicut regions.

Overall in all the ranges, RCP 8.5 receives high precipitation when compared to RCP 4.5. The intensity of precipitation increases towards the northeast and reduces towards the west. The Thirukattipalli and Grand anaicut area located in the western part of the study exhibits very poor precipitation. The same might be attributed to the effect of the northeast monsoon. Further, the research shows substantial interannual variabilities in both scenarios, which might be due to the atmospheric circulation changes (Cha et al. 2016). The analogous spatial precipitation distribution pattern in all ranges might be due to the horizontal resolution of the CORDEX data. An increase in mean positive deviation (50%) with a high-frequency rate compared to mean negative deviation (30%) indicates that the probability for flood is higher than the occurrence of drought in both RCPs.

According to RCP 4.5, the flood will occur during 2022, 2025, 2031, 2033, 2052, 2056, 2065, 2090 and 2092, whereas drought will occur during 2036, 2044, 2054, 2066, 2070, 2084 and 2095. According to RCP 8.5, the flood will occur during 2027, 2039, 2048, 2053, 2057, 2082 and 2093, whereas drought will occur during 2023, 2030, 2034, 2055, 2059, 2062, 2065, 2071, 2091 and 2096. However, the effects of drought will be minimal because of decreased precipitation and the absence of consecutive drought years.

5.0 Summary and Conclusion:

The choice of the bias correction algorithm plays a primary role in assessing the impacts of climate change. This study provides an overview of the various bias correction methods and procedure for evaluating several statistical parameters at the district scale. The improvement was achieved for the control data with all bias correction methods with significant differences. Though all the methods are efficient in correcting the daily mean values, the PT and DM methods can potentially fix the other statistical properties. Further, it is found that the Power transformation method seems to be the best as far as this study area is concerned. The future climate projections of the bias-corrected ensemble show considerable changes throughout the Century. Most of the years will receive heavy precipitation; rather, some years will receive low and average precipitation than observed data. The spatial distribution pattern indicates that the northeast monsoon will dominate over all the ranges and places.

This district is known for paddy cultivation. The projected precipitation will also influence the crop selection, length of the growing period, cropping pattern, crop rotation, crop management practices, sowing period, cropping area extent, agricultural production, and so on. In urban areas, the possibility for land use and land cover changes, ground/river/surface water level changes, flood, soil erosion is high. Further, the study area is also known for heritage and tourism. Thus the study has provided a piece of clear information on future precipitation to the environmentalist, urban planners and policymakers of disaster management. Rainwater harvesting, recharging the aquifers, afforestation, and redirecting the excess amount of water to the river through proper channels are plausible suggestions to overcome excessive precipitation in the future.

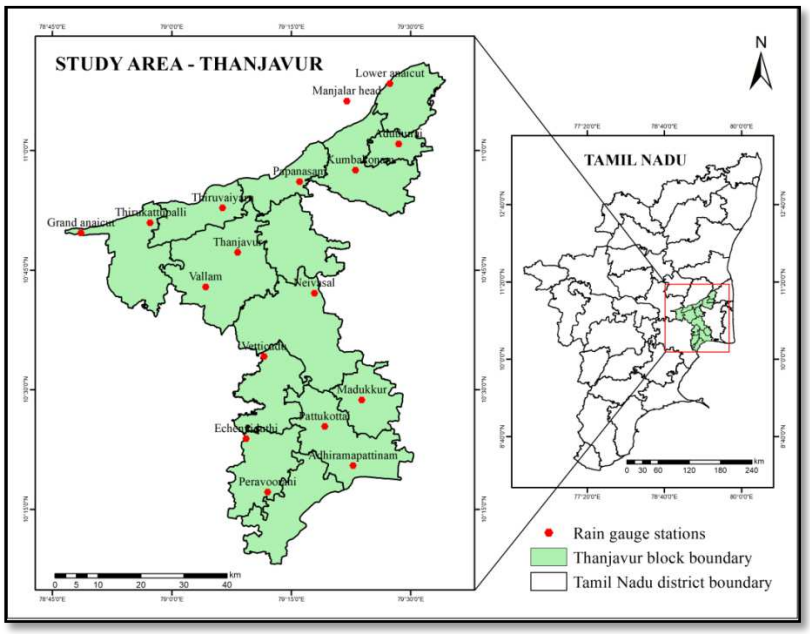

Figure 1. Study area map showing Thanjavur district with block boundary and rain gauge stations

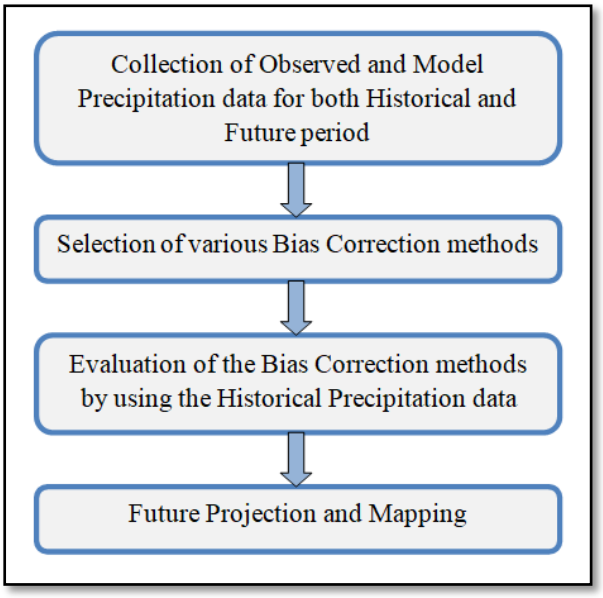

Figure 2. Methodology

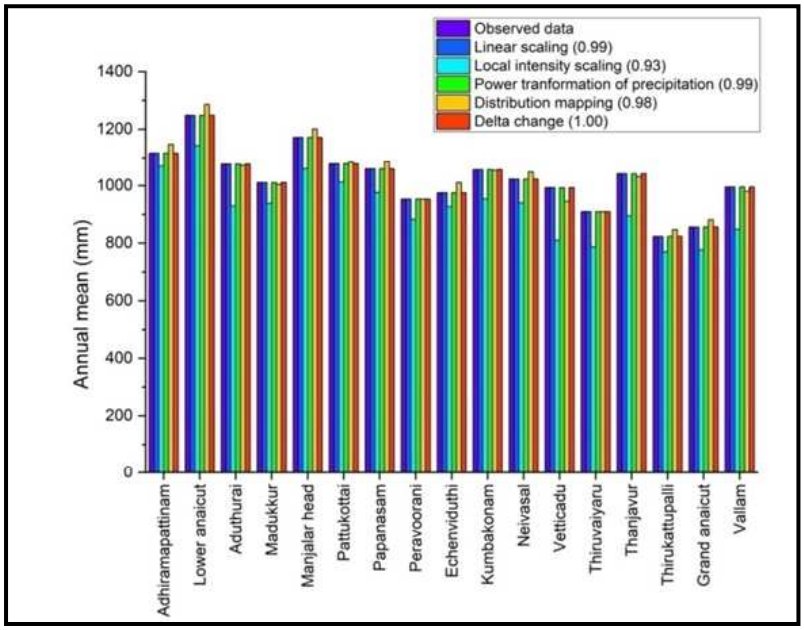

Figure 3. Graphical representation of annual mean precipitation distribution of observed and bias corrected control data for various bias correction methods with the resulted correlation coefficient

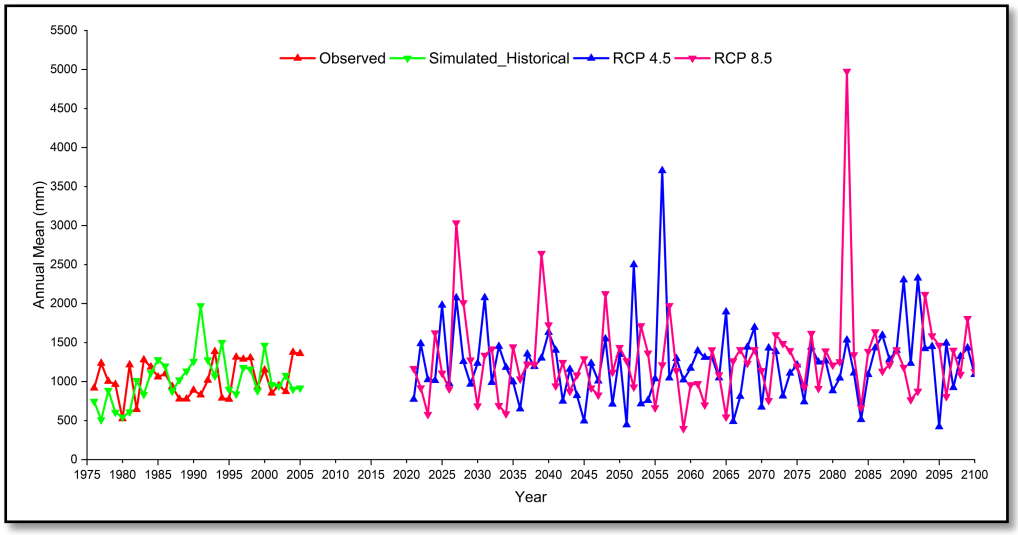

Figure 4. Plot showing time series annual mean precipitation (mm) for the observed, adjusted control and the RCP scenarios in Thanjavur district.

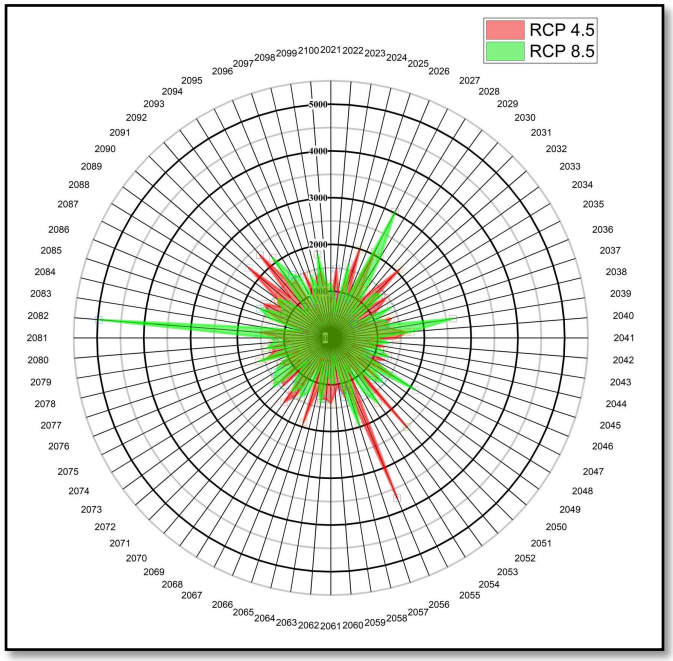

Figure 5. The wind rose diagram showing the temporal distribution pattern of annual mean precipitation for RCP 4.5 and RCP 8.5 (2021 to 2100)

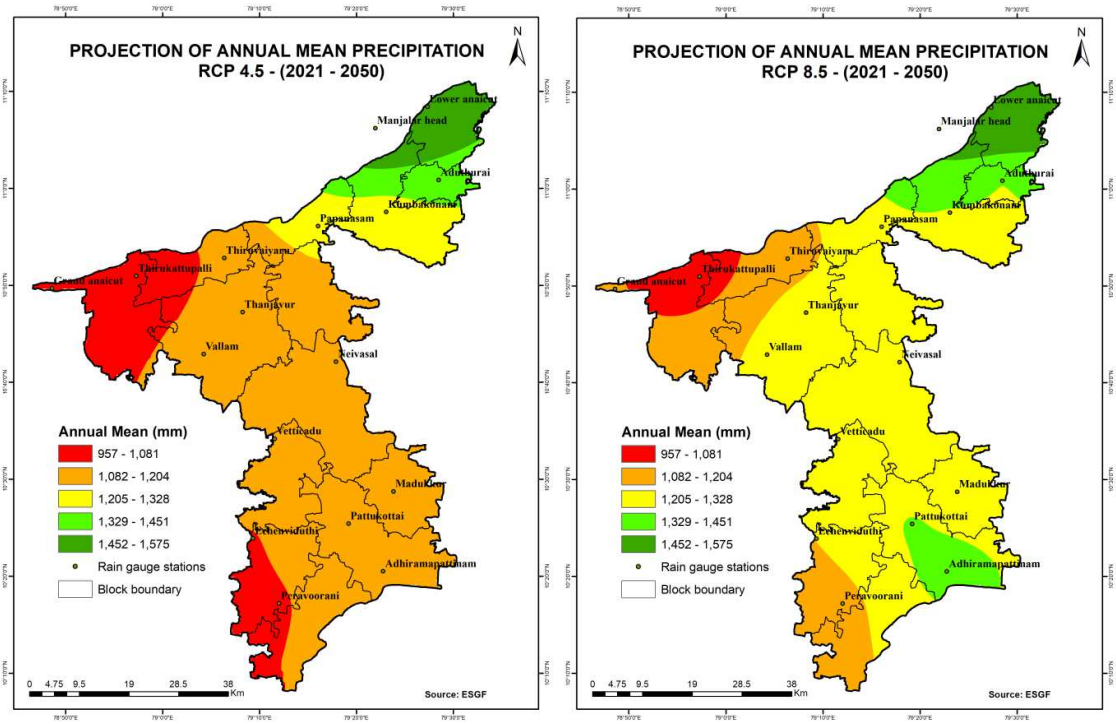

Figure 6. Map showing the spatial distribution pattern of annual mean precipitation for RCP 4.5 and RCP 8.5 in the near range period (2021-2050)

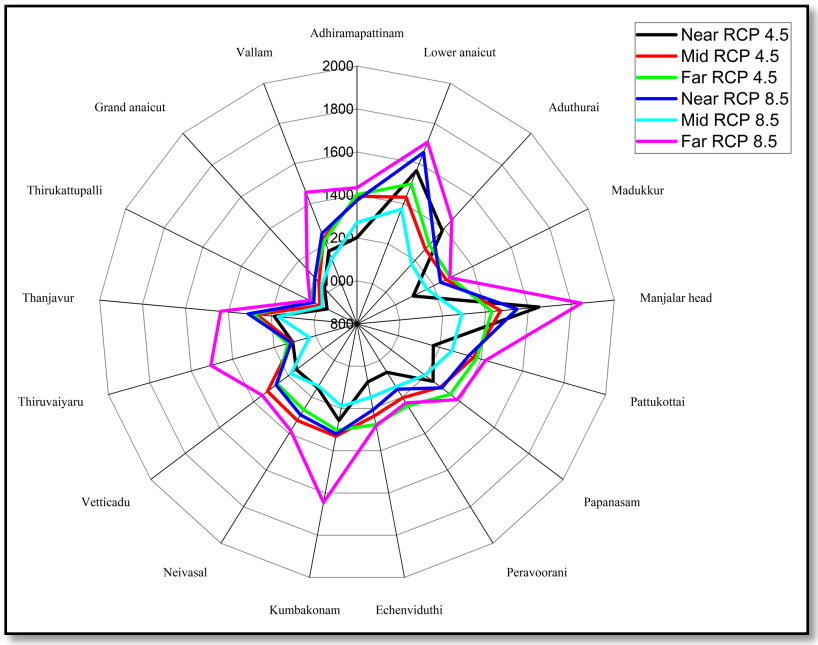

Figure 7. The wind rose diagram showing annual mean precipitation for both RCP scenarios in all three-time ranges

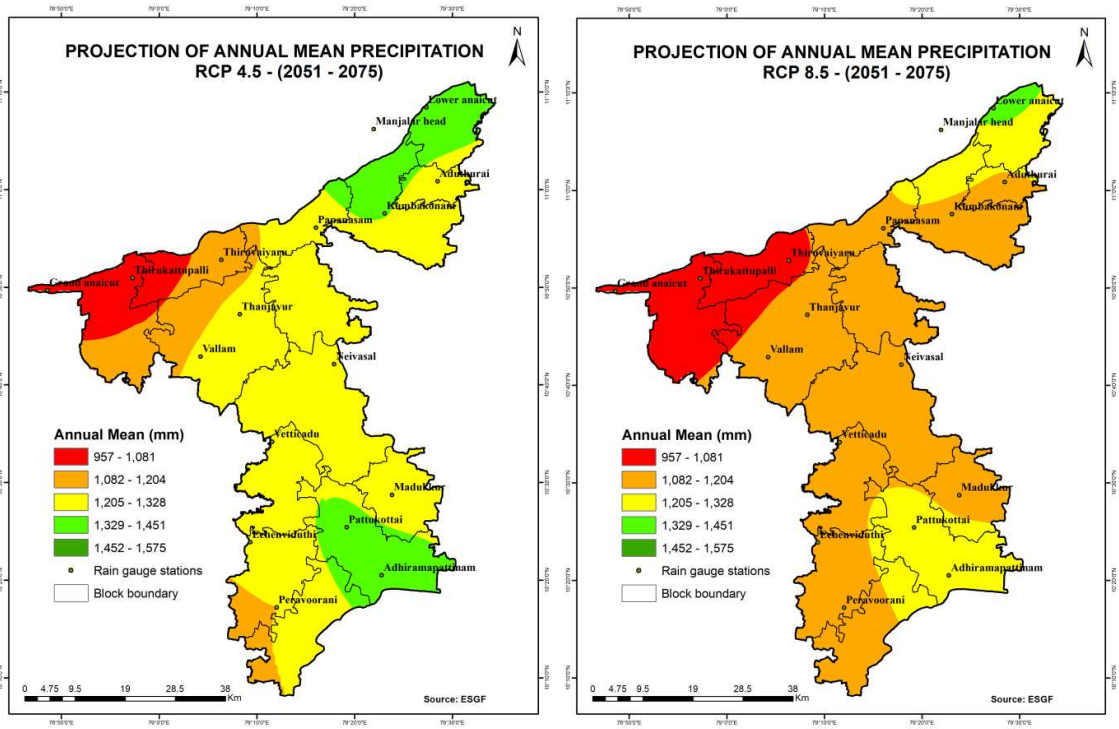

Figure 8. Map showing the spatial distribution pattern of annual mean precipitation for RCP 4.5 and RCP 8.5 in the mid range period (2051-2075)

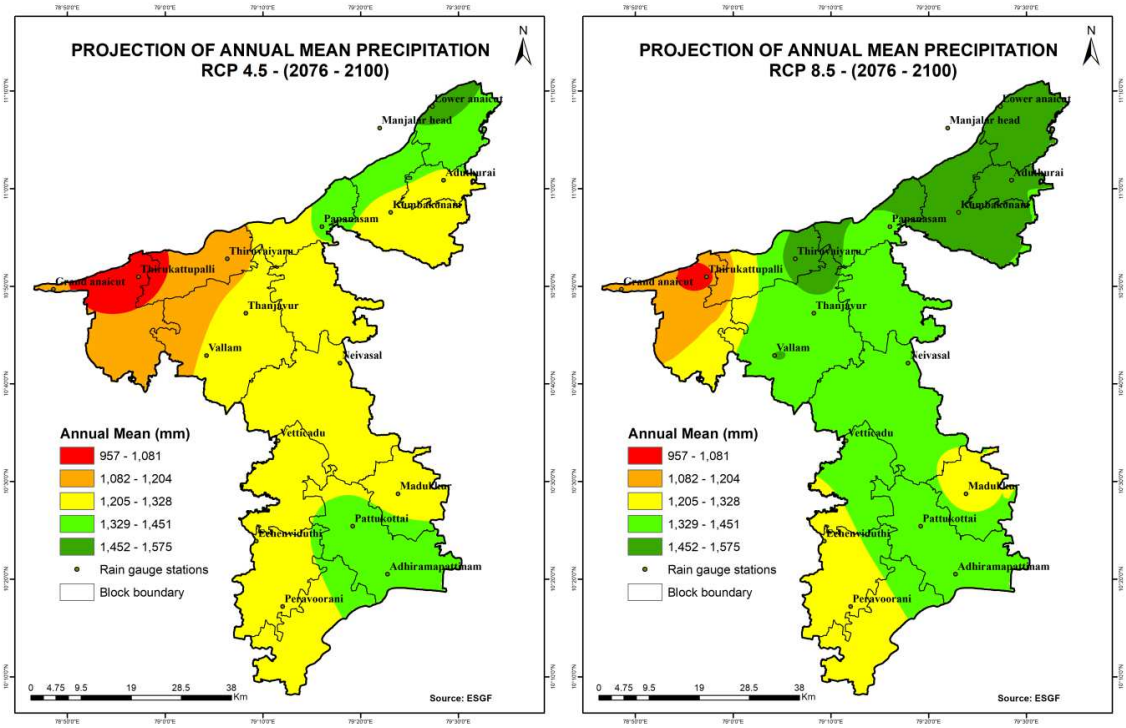

Figure 9. Map showing the spatial distribution pattern of annual mean precipitation for RCP 4.5 and RCP 8.5 in the far range period (2076-2100)

Declarations:

Conflict of Interest

The authors have no conflicts of interest to declare that are relevant to the content of this manuscript.

Funding Statement

The authors did not receive support from any organization for the submitted work.

Author's Contribution

R. Selvakumar: Conceptualization, Methodology, Writing - review and editing, Supervision

S. Gunavathi: Analysis and investigation, Writing - original draft preparation

Availability of data and material

The datasets generated during and/or analysed during the current study are available from the corresponding author on reasonable request.

Code availability

Not applicable

Ethics approval

Not applicable

Consent to participate

Not applicable

Consent for publication

Not applicable

References:

Alexander, L., Allen, S., & Bindoff, N. L. (2013) Working group I contribution to the IPCC fifth assessment report climate change 2013: The physical science basis summary for policymakers (No. Bajados de Internet/2013). OPCC.

Bennett, J. C. et al. (2011) Performance of Quantile-Quantile Bias-Correction for Use in Hydroclimatological Projections. *MODSIM 2011 - 19th International Congress on Modelling and Simulation - Sustaining Our Future: Understanding and Living with Uncertainty* (December), 2668–75.

Brent, R.P., (1971) An algorithm with guaranteed convergence for finding a zero of a function. Comput. J. 14 (4), 422-425. http://dx.doi.org/10.1093/comjnl/14.4.422.

Cha, D. H., Lee, D. K., Jin, C. S., Kim, G., Choi, Y., Suh, M. S., ... & Kang, H. S. (2016) Future changes in summer precipitation in regional climate simulations over the Korean Peninsula forced by multi-RCP scenarios of HadGEM2-AO. Asia-Pacific Journal of Atmospheric Sciences, 52(2), 139-149.

Chen, J., Brissette, F.P., Poulin, A., Leconte, R., (2011b) Overall uncertainty study of the hydrological impacts of climate change for a Canadian watershed. Water

Chen J, Brissette FP, Chaumont D, Braun M. (2013) Finding appropriate bias correction methods in downscaling precipitation for hydrologic impact studies over North America. Water Resour. Res. 49: 4187-4205. https://doi.org/10.1002/wrcr.20331.

Christensen, J.H., Boberg, F., Christensen, O.B., Lucas-Picher, P., (2008) On the need for bias correction of regional climate change projections of temperature and precipitation. Geophys. Res. Lett. 35 (20), L20709. http://dx.doi.org/10.1029/2008GL035694.

Devi, Usha, M. S. Shekhar, and G. P. Singh. (2021) Correction of Mesoscale Model Daily Precipitation Data over Northwestern Himalaya. *Theoretical and Applied Climatology,* 143(1–2), 51–60.

Dosio A, Paruolo P (2011) Bias correction of the ENSEMBLES highresolution climate change projections for use by impact models: Evaluation on the present climate. J Geophys Res 116. https://doi.org/10.1029/2011jd015934

Giorgi F, Mearns LO (1999) Introduction to special section: regional climate modeling revisited. J Geophys Res-Atmos 104:6335-6352. https://doi.org/10.1029/98jd02072

Giorgi F, Jones C, Asrar GR (2009) Addressing climate information needs at the regional level: the CORDEX framework World Meteorological Organization (WMO). Bulletin 58:175

Giorgi, F., & GAO, X. J. (2018) Regional earth system modeling: review and future directions. Atmospheric and Oceanic Science Letters, 11(2), 189-197.

Gudmundsson, L., Bremnes, J. B., Haugen, J. E., & Engen-Skaugen, T. (2012) Downscaling RCM precipitation to the station scale using statistical transformations-a comparison of methods. Hydrology and Earth System Sciences, 16(9), 3383-3390.

Hanel M, Buishand TA (2011) Analysis of precipitation extremes in an ensemble of transient regional climate model simulations for the Rhine basin. Clim Dyn 36:1135-1153. https://doi.org/10.1007/s00382-010-0822-2

Hall, A. (2014) Projecting regional change. Science, 346(6216), 1461-1462. https://doi.org/10.1126/science.aaa0629yar

Ines AVM, Hansen JW. (2006) Bias correction of daily GCM rainfall for crop simulation studies. Agric. For. Meteorol. 138: 44-53. https://doi .org/10.1016/j.agrformet.2006.03.009.

Johnson, C. R., Banks, S. C., Barrett, N. S., Cazassus, F., Dunstan, P. K., Edgar, G. J., ... & Taw, N. (2011)Climate change cascades: Shifts in oceanography, species' ranges and subtidal marine community dynamics in eastern Tasmania. Journal of Experimental Marine Biology and Ecology, 400(1-2), 17-32.

Kim, G., Cha, D. H., Lee, G., Park, C., Jin, C. S., Lee, D. K., ... & Kim, J.(2020) Projection of future precipitation change over South Korea by regional climate models and bias correction methods.

Kumar, P., Wiltshire, A., Mathison, C., Asharaf, S., Ahrens, B., Lucas-Picher, P., ... & Jacob, D. (2013) Downscaled climate change projections with uncertainty assessment over India using a high resolution multi-model approach. Science of the Total Environment, 468, S18-S30.

Lafon, Thomas, Simon Dadson, Gwen Buys, and Christel Prudhomme. (2013) Bias Correction of Daily Precipitation Simulated by a Regional Climate Model: A Comparison of Methods. *International Journal of Climatology,* 33(6), 1367–81.

Mendez, M., Maathuis, B., Hein-Griggs, D., & Alvarado-Gamboa, L. F. (2020) Performance Evaluation of Bias Correction Methods for Climate Change Monthly Precipitation Projections over Costa Rica. Water, 12(2), 482.

Middelkoop, H., Daamen, K., Gellens, D., Grabs, W., Kwadijk, J.C. J., Lang, H., Parmet, B., Schadler, B., Schulla, J., and Wilke,K. (2001) Impact of climate change on hydrological regimes and waterresources management in the Rhine Basin. Clim. Change, 49, 105–128.

Monhart S, Spirig C, Bhend J, Bogner K, Schar C, Liniger MA (2018) Skill of subseasonal forecasts in Europe: effect of bias correction and downscaling using surface observations. J Geophys Res-Atmos 123:7999-8016. https://doi.org/10.1029/2017jd027923

Noguer, M., Jones, R., & Murphy, J. (1998) Sources of systematic errors in the climatology of a regional climate model over Europe. Climate Dynamics, 14(10), 691-712.

N'Tcha M'Po, Yèkambèssoun. (2016) Comparison of Daily Precipitation Bias Correction Methods Based on Four Regional Climate Model Outputs in Ouémé Basin, Benin. *Hydrology,* 4(6), 58.

Piani, C., J. O. Haerter, and E. Coppola. (2010) Statistical Bias Correction for Daily Precipitation in Regional Climate Models over Europe. Theoretical and Applied Climatology, 99(1–2), 187–92.

PontoppidanM, Kolstad EW, Sobolowski S, King MP (2018) Improving the reliability and added value of dynamical downscaling via correction of large-scale errors: a Norwegian perspective. J Geophys Res-Atmos 123:11,875-811,888. https://doi.org/10.1029/2018jd028372

Prusty, R. M., Das, A., & Patra, K. C. (2018) Climate change impact assessment under CORDEX South-Asia RCM scenarios on water resources of the Brahmani and Baitarini River Basin, India.

Rathjens, H., Bieger, K., Srinivasan, R., Chaubey, I., & Arnold, J. G. (2016) CMhyd User Manual.

Räty, Olle, Jouni Räisänen, and Jussi S. Ylhäisi. (2014) Evaluation of Delta Change and Bias Correction Methods for Future Daily Precipitation: Intermodel Cross-Validation Using ENSEMBLES Simulations. *Climate Dynamics,* 42(9–10), 2287–2303.

Rauscher, S. A., Coppola, E., Piani, C., & Giorgi, F. (2010) Resolution effects on regional climate model simulations of seasonal precipitation over Europe. Climate dynamics, 35(4), 685-711

Schmidli, J., Frei, C., & Vidale, P. L. (2006) Downscaling from GCM precipitation: a benchmark for dynamical and statistical downscaling methods. International Journal of Climatology: A Journal of the Royal Meteorological Society, 26(5), 679-689.

Schulzweida, Uwe. (2019) CDO User Guide (Version 1.9.8). http://doi.org/10.5281/zenodo.3539275).

Shrestha, Durga Lal, David E. Robertson, James C. Bennett, and Q. J. Wang. (2015) Improving Precipitation Forecasts by Generating Ensembles through Postprocessing. *Monthly Weather Review,* 143(9), 3642–63.

Terink, W, R T W L Hurkmans, P J J F Torfs, and R Uijlenhoet (2009) Bias Correction of Temperature and Precipitation Data for Regional Climate Model Application to the Rhine Basin. Hydrology and Earth System Sciences Discussions, 6(4), 5377–5413.

Teutschbein C, Seibert J (2012) Bias correction of regional climate model simulations for hydrological climate-change impact studies: review and evaluation of different methods. J Hydrol 456:12-29. https:// doi.org/10.1016/j.jhydrol.2012.05.052

Teutschbein, C., & Seibert, J. (2013) Is bias correction of regional climate model (RCM) simulations possible for non-stationary conditions?. Hydrology and Earth System Sciences, 17(12), 5061-5077.

Themeßl, M. J., Gobiet, A., & Heinrich, G. (2012) Empirical-statistical downscaling and error correction of regional climate models and its impact on the climate change signal. Climatic Change, 112(2), 449-468.

Van Vuuren DP et al (2011) The representative concentration pathways: an overview. Clim Change, 109:5-31. https://doi.org/10.1007/ s10584-011-0148-z.

Veijalainen N, Lotsari E, Alho P, Vehviläinen B, Käyhkö J (2010) National scale assessment of climate change impacts on flooding in Finland. J Hydrol 391:333-350.

Figures

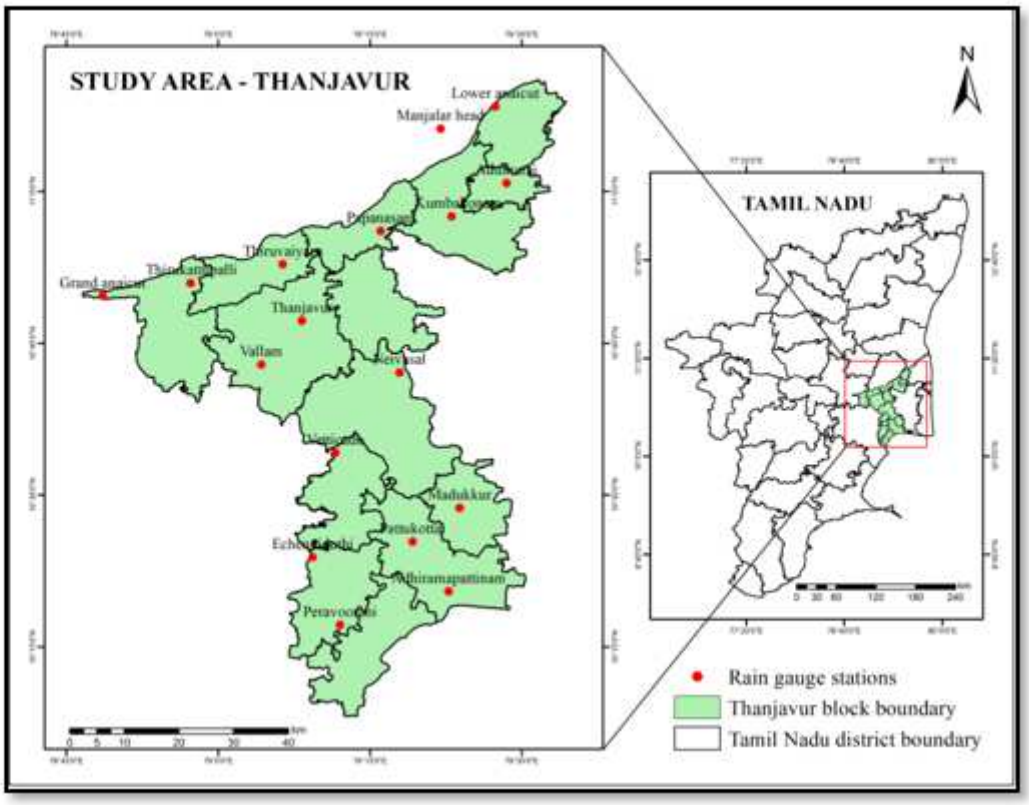

Figure 1

Study area map showing Thanjavur district with block boundary and rain gauge stations. Note: The designations employed and the presentation of the material on this map do not imply the expression of any opinion whatsoever on the part of Research Square concerning the legal status of any country, territory, city or area or of its authorities, or concerning the delimitation of its frontiers or boundaries. This map has been provided by the authors.

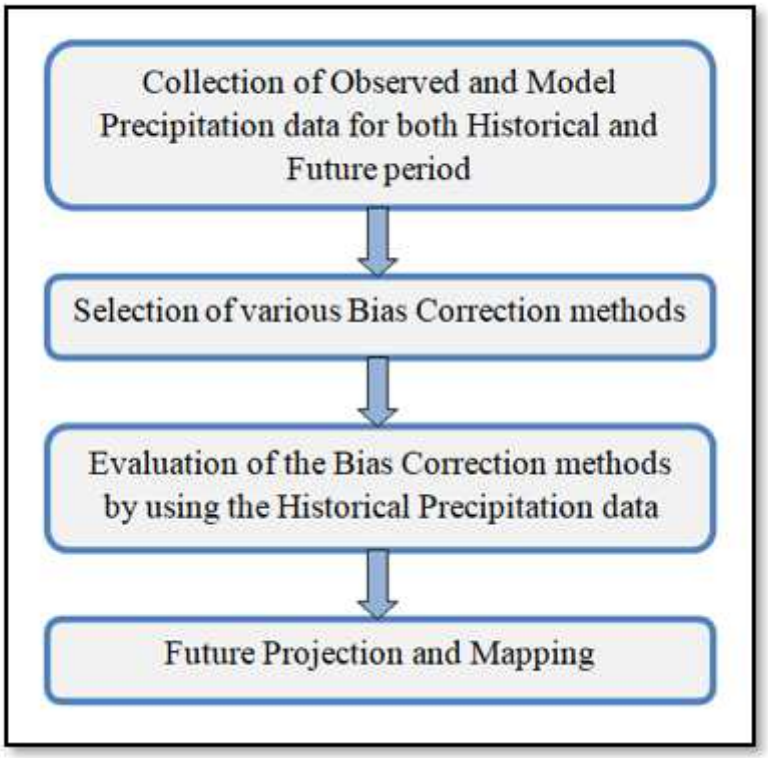

Figure 2

Methodology

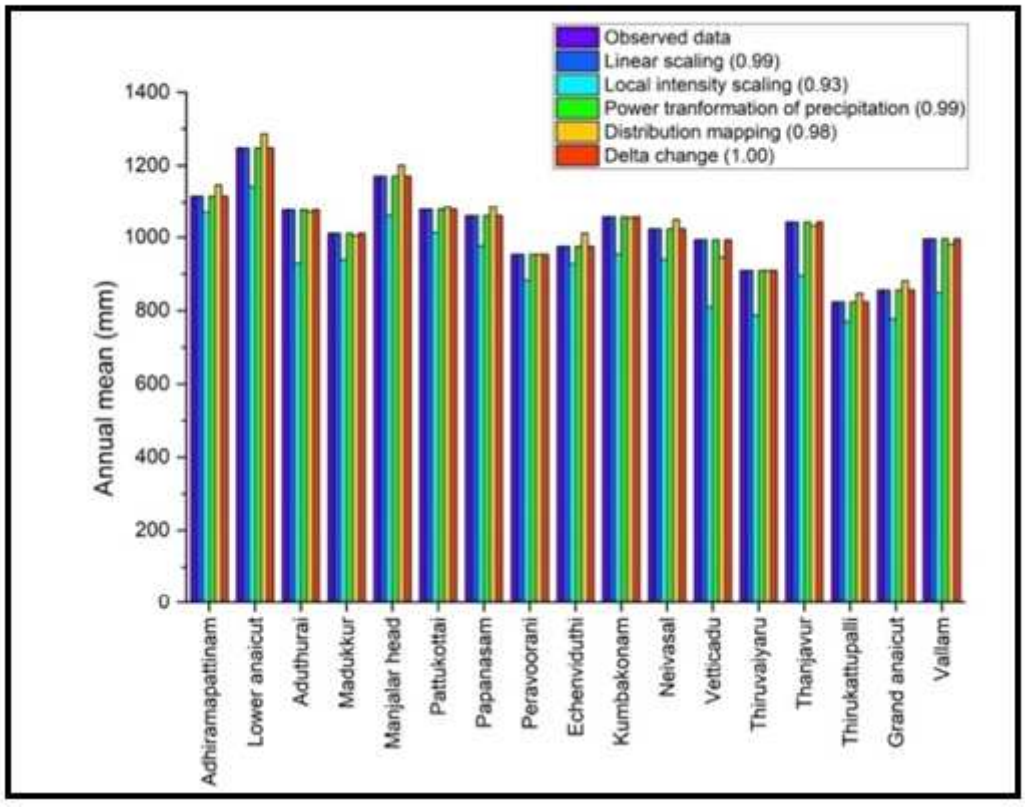

Figure 3

Graphical representation of annual mean precipitation distribution of observed and bias corrected control data for various bias correction methods with the resulted correlation coefficient

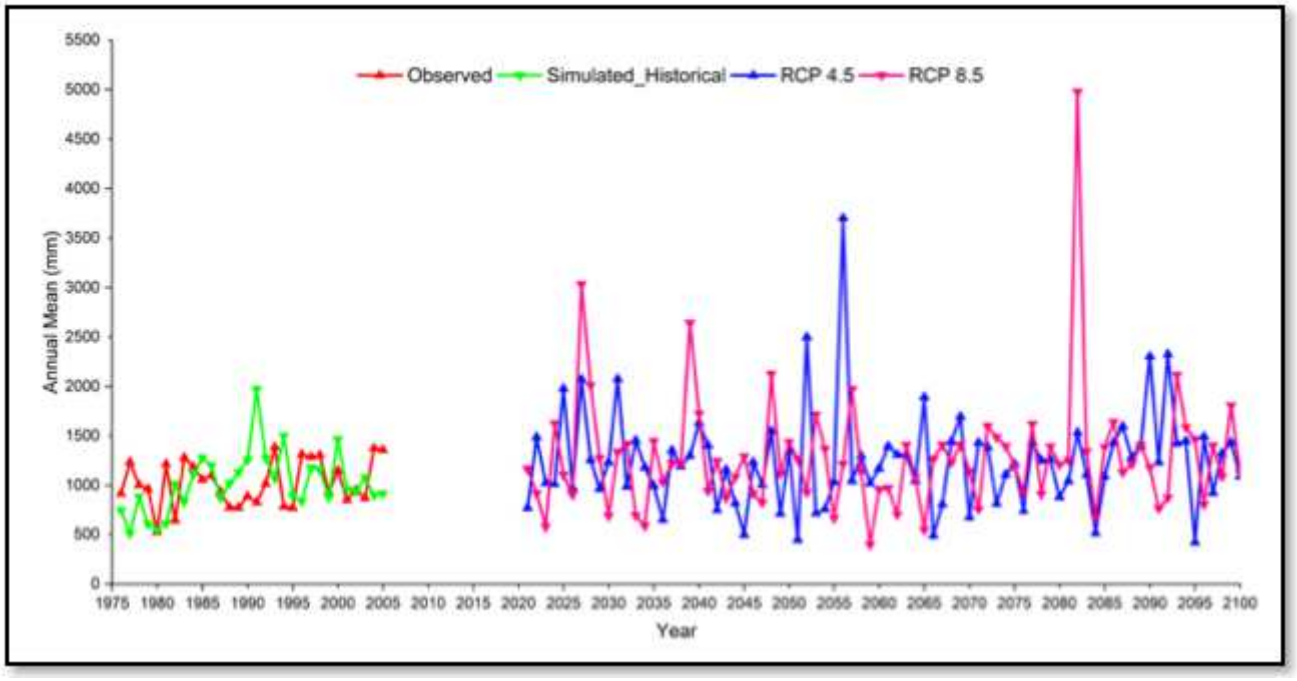

Figure 4

Plot showing time series annual mean precipitation (mm) for the observed, adjusted control and the RCP scenarios in Thanjavur district.

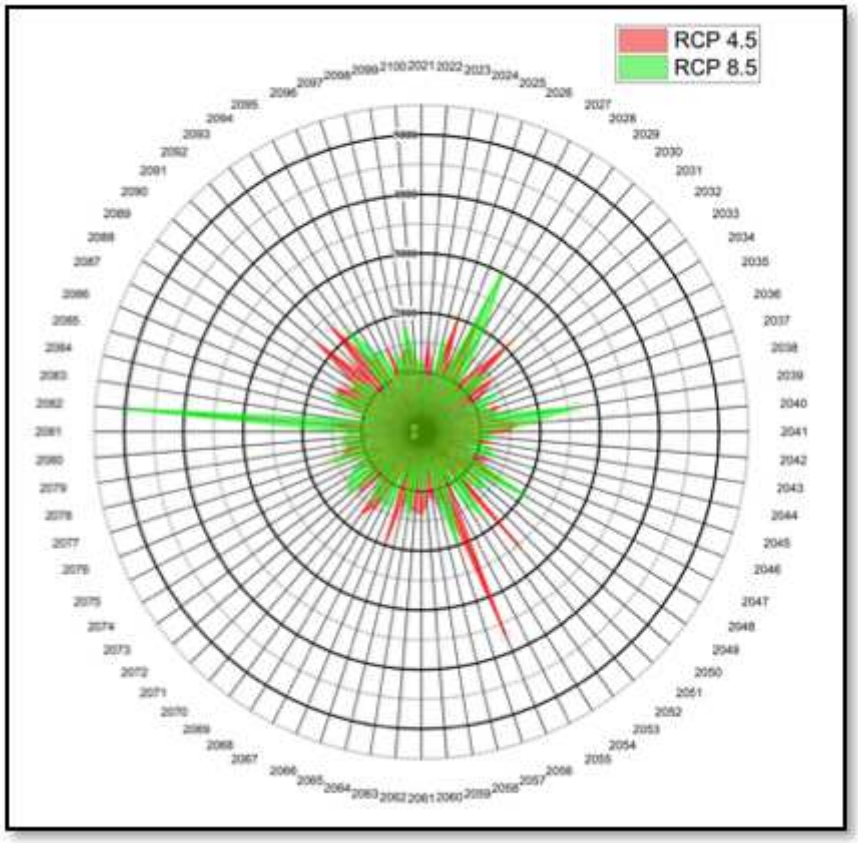

Figure 5

The wind rose diagram showing the temporal distribution pattern of annual mean precipitation for RCP 4.5 and RCP 8.5 (2021 to 2100)

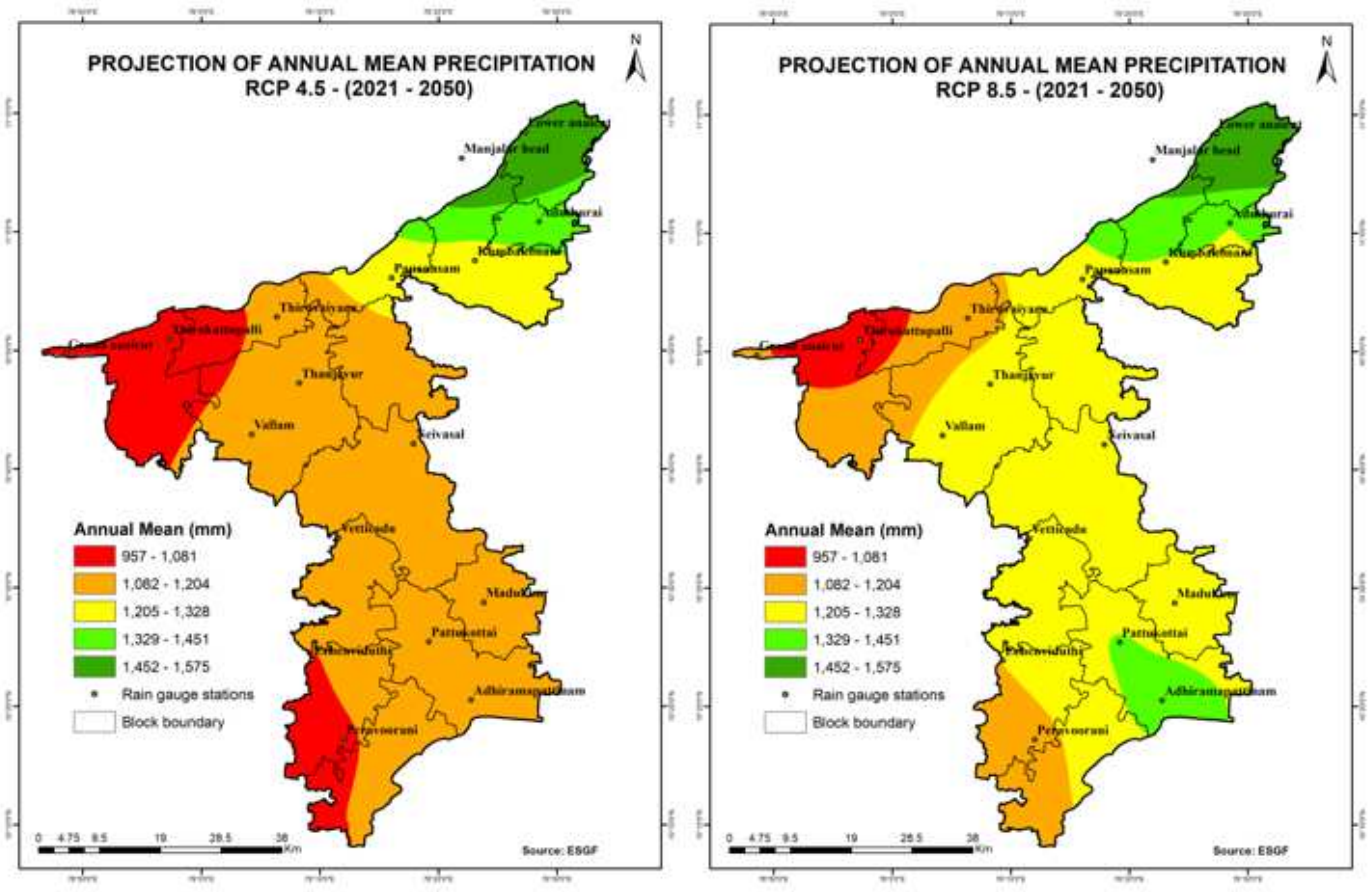

Figure 6

Map showing the spatial distribution pattern of annual mean precipitation for RCP 4.5 and RCP 8.5 in the near range period (2021-2050). Note: The designations employed and the presentation of the material on this map do not imply the expression of any opinion whatsoever on the part of Research Square concerning the legal status of any country, territory, city or area or of its authorities, or concerning the delimitation of its frontiers or boundaries. This map has been provided by the authors.

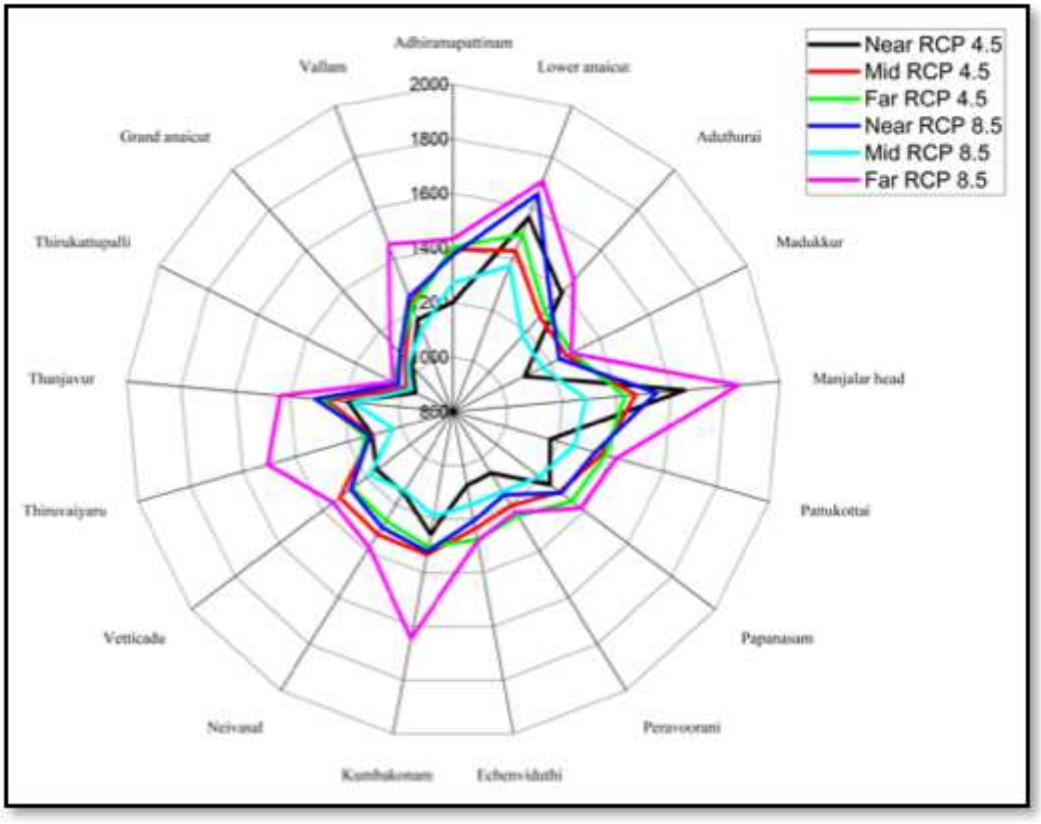

Figure 7

The wind rose diagram showing annual mean precipitation for both RCP scenarios in all three-time ranges

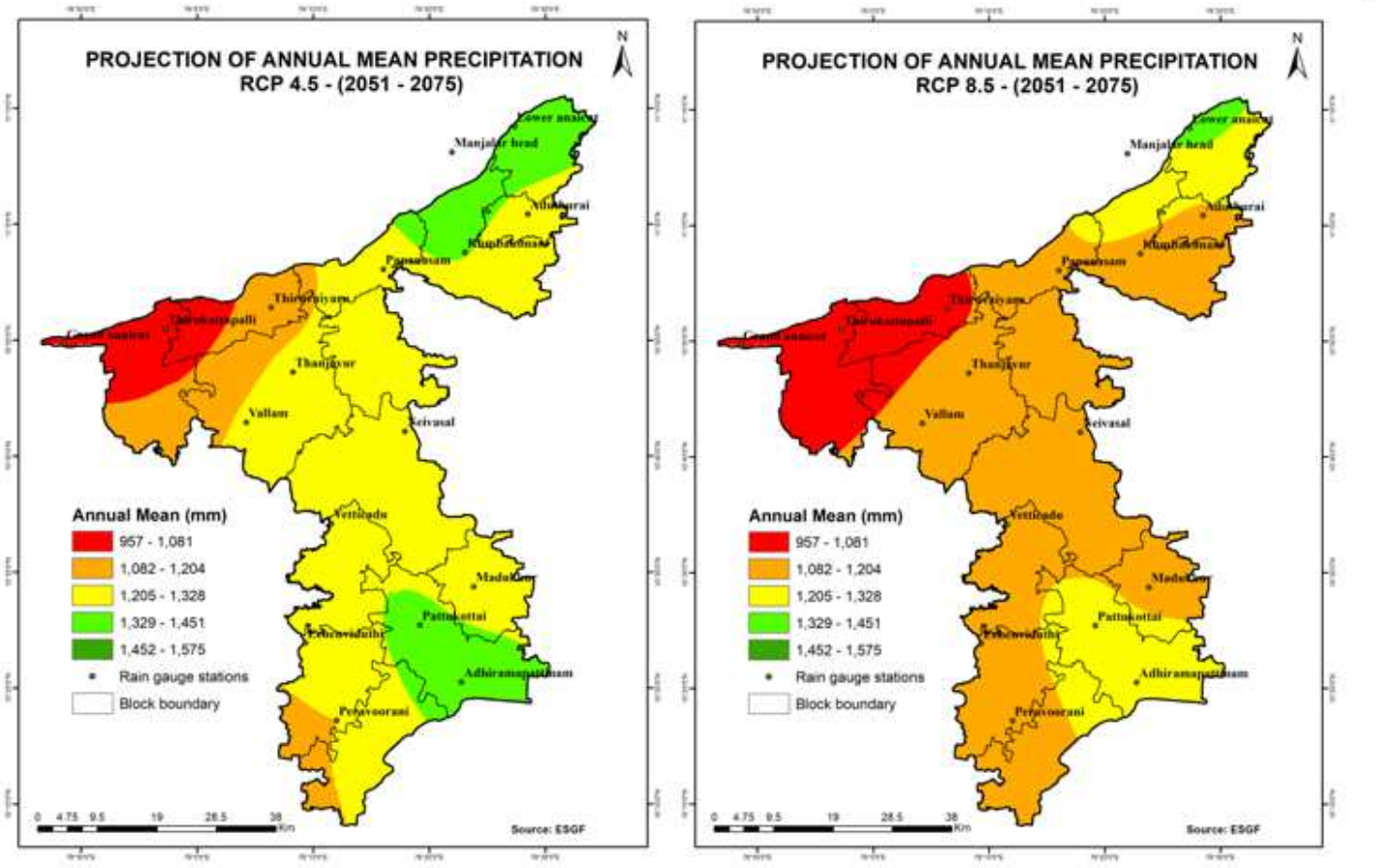

Figure 8

Map showing the spatial distribution pattern of annual mean precipitation for RCP 4.5 and RCP 8.5 in the mid range period (2051-2075). Note: The designations employed and the presentation of the material on this map do not imply the expression of any opinion whatsoever on the part of Research Square concerning the legal status of any country, territory, city or area or of its authorities, or concerning the delimitation of its frontiers or boundaries. This map has been provided by the authors.

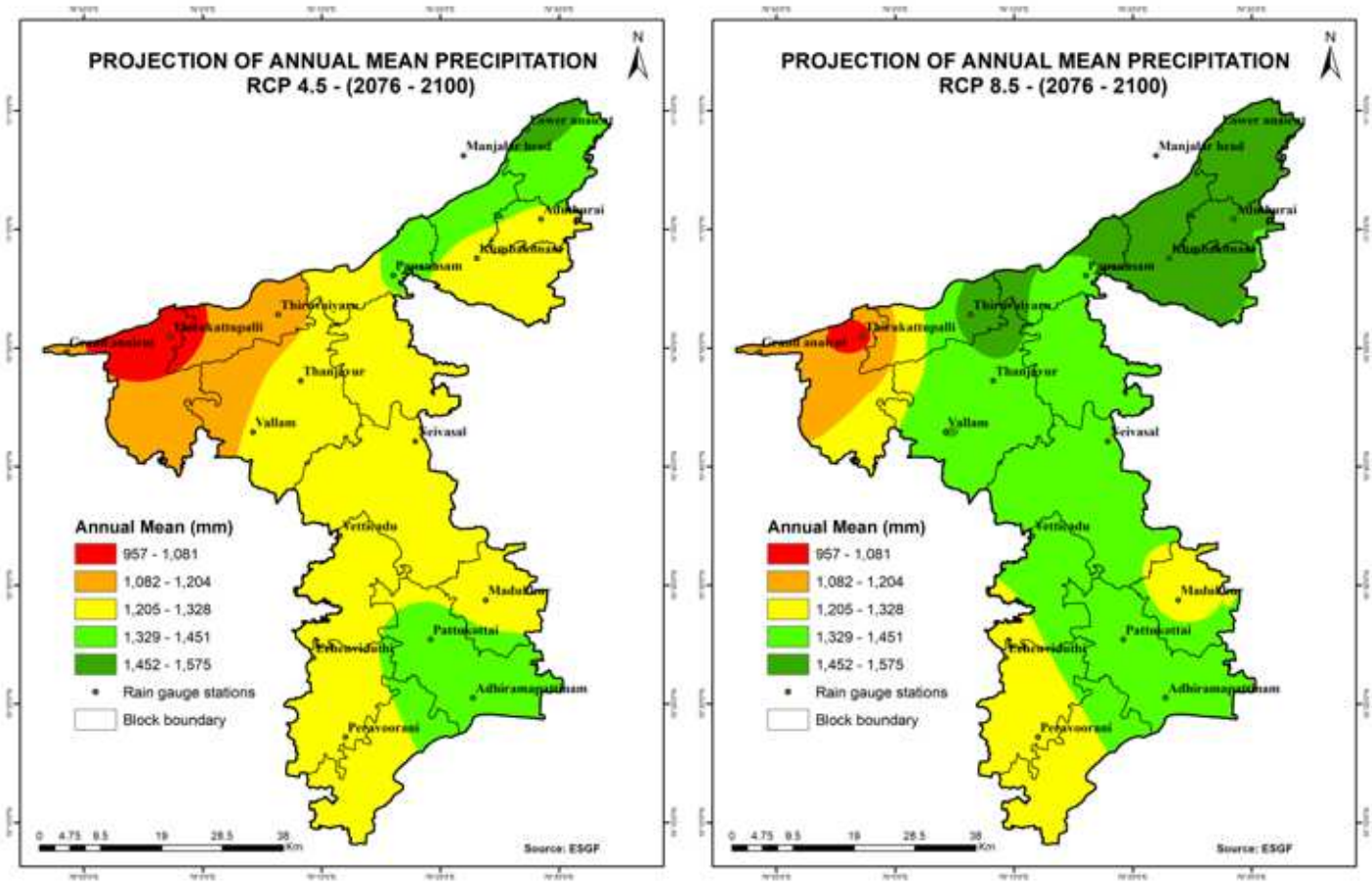

Figure 9

Map showing the spatial distribution pattern of annual mean precipitation for RCP 4.5 and RCP 8.5 in the far range period (2076-2100). Note: The designations employed and the presentation of the material on this map do not imply the expression of any opinion whatsoever on the part of Research Square concerning the legal status of any country, territory, city or area or of its authorities, or concerning the delimitation of its frontiers or boundaries. This map has been provided by the authors.